As of 10 June 2016

This GOES-R Level 2+ space weather Algorithm Theoretical Basis Document (ATBD) is preliminary and subject to change as the GOES-R Program prepares for a launch in late 2016.

The NOAA National Centers for Environmental Information (NCEI) is currently developing a demonstration version of the Satellite Product Analysis and Distribution Enterprise System (SPADES) which will host the L2+ algorithms. The operational SPADES will be instantiated by the National Weather Service in FY2017 to serve the needs of the Space Weather Prediction Center (SWPC).

Updated versions of the L2+ ATBDs will periodically be made available and posted to the SPADES website.

Bill Denig
NCEI

http://www.ngdc.noaa.gov/stp/space-weather/online-publications/stp_sii/spades/

NOAA NESDIS CENTER for SATELLITE APPLICATIONS and RESEARCH

MAGNETOMETER MAGNETOPAUSE CROSSING DETECTION ALGORITHM THEORETICAL BASIS DOCUMENT
Version 1.0

Hardcopy Uncontrolled

TITLE: MAGNETOMETER MAGNETOPAUSE CROSSING DETECTION ALGORITHM THEORETICAL BASIS DOCUMENT VERSION 1.0

AUTHORS:
Dr. Paul Lotoaniu
Dr. Howard Singer
Mark Berguson

APPROVAL SIGNATURES:

_____<Actual Signature Date>
<Name of Technical Approver> Date
Technical Approver

_____<Actual Signature Date>
<Name of Agency Approver> Date
Agency

MAG MAGNETOPAUSE CROSSING DETECTION ALGORITHM
THEORETICAL BASIS DOCUMENT VERSION HISTORY SUMMARY

Version	**Description**	**Revised Sections**	**Date**
1.0	Created by Dr. Paul Lotoaniu CIRES/SWPC	New Document	April 11, 2008

LIST OF FIGURES 9
List of Tables 10
LIST OF ACRONYMS 11
ABSTRACT 12
1.1 Purpose of This Document 13
1.2 Who Should 13
Use This Document 13
1.3 Inside Each Section 13
1.4 Related Documents 14
1.5 Revision History 14
2.0 OBSERVING SYSTEM OVERVIEW 14
2.1 Product Generated 14
2.2 Instrument Characteristics 15
3.0 ALGORITHM DESCRIPTION 15
3.1 Algorithm Overview 15
3.2 Processing Outline 16
3.3 Algorithm Input 17
3.3.1 Primary Sensor Data 17
3.3.2 Ancillary Data 18
3.4 Theoretical Description 18
3.4.1 Physics of the Problem 19
3.4.2 Mathematical Description 23
3.4.3 Algorithm Output 26
4.0 TEST DATA SETS AND OUTPUTS 27
4.1 Simulated/Proxy Input Data Sets 27
4.2 Output from Simulated/Proxy Inputs Data Sets 27
4.2.1 Output from MAG and SEISS simulated inputs data sets 27
4.2.2 Output from magnetopause model tests 29
4.2.3 Output example from full algorithm 31
4.2.4 Precisions and Accuracy Estimates 32
4.2.2 Error Budget 33
5.0 PRACTICAL CONSIDERATIONS 33
5.1 Numerical Computation Considerations 33
5.2 Programming and Procedural Considerations 33
5.3 Quality Assessment and Diagnostics 34
5.4 Exception Handling 34
5.5 Algorithm Validation 34
6.0 ASSUMPTIONS AND LIMITATIONS 34
6.1 Performance 34
6.2 Assumed Sensor Performance 35

6.3 Pre-Planned Product Improvements 35
6.3.1 Improvement 1 35
6.3.2 Improvement 2 35
6.3.3 Improvement 3 35
6.3.4 Improvement 4 35
6.3.5 Improvement 5 36
6.3.6 Improvement 6 36
7.0 REFERENCES 36

LIST OF FIGURES

Figure 1 High-level flowchart of the GMC detection algorithm. 16
Figure 2 High-level flowchart of the magnetic local time (MLT) processing outline..... 17
Table 1 Sensor input data to the algorithm 17
Table 2 Ancillary input data to the algorithm 18
Figure 3 Shown is an example GMC detected by the GOES 6 & 7 magnetometers..... 19
Figure 4 Shows the change is different parameters as the ISEE spacecraft moves from the magnetosphere to the magnetospheath (outside the magnetosphere). The density and temperature after the second vertical red line is significantly different to the values before the first red vertical line. 21
Table 3 test results of comparisons between the three different magnetopause models. . 23
Table 4 Algorithm output..... 26
Figure 5 Output examples of two different GMC events when LANL and GOES were 30 degrees apart (top panels) and when LANL and GOES were 90 degrees apart. The number of particle flags that agree with magnetometer flags significantly decrease when the spacecraft are separated by 90 degrees. 28
Figure 6 An output example from magnetopause model component of algorithm showing how the r-vector flags can disagree with magnetic field component of the algorithm..... 29
Figure 7 Output examples from magnetopause model component of algorithm showing disagreemtn in the r-vector flags (left panels) and errors in the flags. 30
Figure 8 Example output with no errors. From top to bottom panels are HP the Hp-compnent of GOES magnetic field observations, magnetic field Flag, PIR is the ion density to temperature, ion ration event flag, PER is the electron density to temperature ratio, electron event flag, magnetopause model r_0-vector, r_0-vector event flag, magnetopause model r-vector, r-vector event flag and MLT. 31
Figure 9 Example output with errors. From top to bottom panels are HP the Hp-compnent of GOES magnetic field observations, magnetic field Flag, PIR is the ion density to temperature, ion ration event flag, PER is the electron density to temperature ratio, electron event flag, magnetopause model r_0-vector, r_0-vector event flag, magnetopause model r-vector, r-vector event flag and MLT. 32

List of Tables

Table 1 Sensor input data to the algorithm 17
Table 2 Ancillary input data to the algorithm 18
Table 3 test results of comparisons between the three different magnetopause models. . 23
Table 4 Algorithm output 26

LIST OF ACRONYMS

ATBD	Algorithm Theoretical Basis Document
CIRES	Cooperative Institute for Research in Environmental Sciences
MAG	Magnetometer
STAR	Center for Satellite Applications and Research
SWPC	Space Weather Prediction Center
GMC	Geosynchronous magnetopause crossing
MP	Magnetopause

ABSTRACT

The algorithm determines whether the GOES spacecraft has crossed the magnetopause. It accomplishes this by determining three conditions: (1) whether the north-south magnetic field component measured by GOES is less than zero, (2) whether there is a substantial increase in the mid-energy ion and electron density to temperature ratios and (3) whether the Shue et al. (1998) magnetopause model r-vector (the magnetopause location along the Earth-satellite vector) and r_0-vector (the magnetopause subsolar standoff distance along the Earth-sun line) is less than 6.6 R_E (geosynchronous altitude). This ATBD provides a mathematical and pseudo code description of the algorithm. The assumptions made regarding input spacecraft attitude data and ephemerides are also described. Example test runs using proxy data are shown and compared to results from currently implemented algorithms. Current algorithm limitations and possible future improvements are also discussed.

1.0 INTRODUCTION

1.1 Purpose of This Document

The purpose of this document is to describe the product algorithm and its theoretical basis. This document can be used as a reference for implementing the algorithm into software. The magnetopause crossings detection product uses magnetometer data in the appropriate geophysical coordinate systems to detect when the GOES spacecraft has crossed the magnetopause boundary. The assumptions made regarding input data, instrumentation and input spacecraft attitude are specified. Given that GOES-R orbits at geosynchronous altitudes, in this document we will often refer to magnetopause crossings as GMCs (geosynchronous magnetopause crossings).

1.2 Who Should

Use This Document

The STAR AIT group shall use this document to integrate the algorithm into their collaborative framework environment. It shall also be used by the prime development and implementation contractor to design, develop, test, validate and implement the algorithm into the final operational processing system. In addition, the GOES-R AWG space weather application team shall use this ATBD to verify their operational requirements are being met by the proposed algorithm. They should also use it to understand the strengths and weaknesses of the algorithm as well as its accuracy and applicability.

1.3 Inside Each Section

Section 2.0, OBSERVING SYSTEM OVERVIEW, describes the product objectives and requirements, and assumptions made regarding the magnetometer and SEISS instrument characteristics.

Section 3.0 ALGORITHM DESCRIPTION, describes the theoretical basis of the algorithm, assumptions made for sensory data, input data and ancillary data, algorithm input/output, error estimates and programming, procedural and computational considerations.

Section 4.0 TEST DATA SETS AND OUTPUTS, describes the test data sets used to characterize the performance of the algorithm and the data product quality. Also are described are the results from the algorithm processing on simulated input data.

Section 5.0 PRACTICAL CONSIDERATIONS, discusses issues involving numerical computation, programming and procedures, quality assessment and diagnostics and exception handling.

Section 6.0 ASSUMPTIONS AND LIMITATIONS, discusses algorithm performance with regard to accuracy and the limitations of the algorithm and possible improvements.

Section 7.0 REFERENCES, provides all references mentioned in the ATBD.

1.4 Related Documents

(1) GOES-R MAGNETOMETER PORD (417-R-MAGPORD).

(2) GOES-R Series SEISS PORD (417-R-SEISSPORD-0030).

(3) GOES-R Mission Requirements Document 2B Prime (MRD-2B').

1.5 Revision History

Revision Number	Date	Author	Revision Description	Reason for Revision
2	11 Feb 2011	Paul Loto'aniu		Update from CDR

2.0 OBSERVING SYSTEM OVERVIEW

2.1 Product Generated

The GOES-R GMC detection algorithm is composed of three parts with one using magnetometer data, second using particle data and the third using solar wind data to determine when the GOES-R spacecraft has crossed the magnetopause boundary. The form of the output will be flags (state machine) attached to the data stream that indicates the state of each part of the algorithm with state 1 = magnetopause crossing and state 0 = no magnetopause crossing.

With three parts there are a total of five output flags which are described in more details in section 3.0.

2.2 Instrument Characteristics

The SEISS and MAG instrument operational requirements and characteristics are detailed in sections 3.4.2.5 and 3.4.2.7, respectively, of the GOES-R Series Mission Requirements Document (MRD) Version 3.0 dated February 2007 and the SEISS and MAG instrument Performance and Operational Requirements Documents (PORDs) draft dated in March and November 2004, respectively. The accuracy of the MAG and SEISS components of the algorithm relies on precise instrument orientation and calibration, data timing and knowledge of spacecraft attitude and location. For the magnetopause model component, accuracy is restricted to the inherent accuracy of the model and accuracy of the solar wind data inputted to the model. Algorithm development by the SWx AT will assume the SEISS and MAG instruments meet the performance requirements outlined in the GOES-R MRD and MAG and SEISS PORDs.

3.0 ALGORITHM DESCRIPTION

3.1 Algorithm Overview

The algorithm consists of 3 components:

1. ***Magnetic field***
    - The condition $H_p < H_{p_limit}$ is used to define a GMC. Here, H_p is the north-south magnetic field component in ENP coordinates. The value of H_{p_limit} is based on the correlation between H_p and IMF-B_z during GMCs.
    - It is assumed that GMCs occur only when IMF-B_z is negative, hence, H_{p_limit} *is set to* 0 nT.
2. ***Particle***
    - A substantial increase in the mid-energy ion and electron density (*D*) to temperature (*T*) ratios is used to define a GMC. We use the method defined by Suvorova et al. (2005). Suvorova et al. estimated the ratios using data from 130 *eV/q* to 45 *keV/q energy ions* and 30 *eV* to 45 *keV* electrons. For the GMC algorithm the temperature and density moments are

calculated using the GOES-R mid-energy range (30 eV to 30 keV) data for both electrons and ions.

3. ***Magnetopause model***
   - Three magnetopause models were tested and from these tests we selected the Shue et al. (1998) model for the GMC algorithm. The model requires solar wind magnetic field and dnamic pressure data.

4. ***Algorithm output***
   - There are five output flags and magnetic local time is also an output. There is one flag for the magnetic field component, two flags for particle component and two flags for the model.

3.2 Processing Outline

The processing outline of the GMC detection algorithm is summarized in the Figures 1 and 2 below. The current algorithms are implemented as C++ routines with an object oriented emphasis. However, current maturity does not meet ISO 2003 standard.

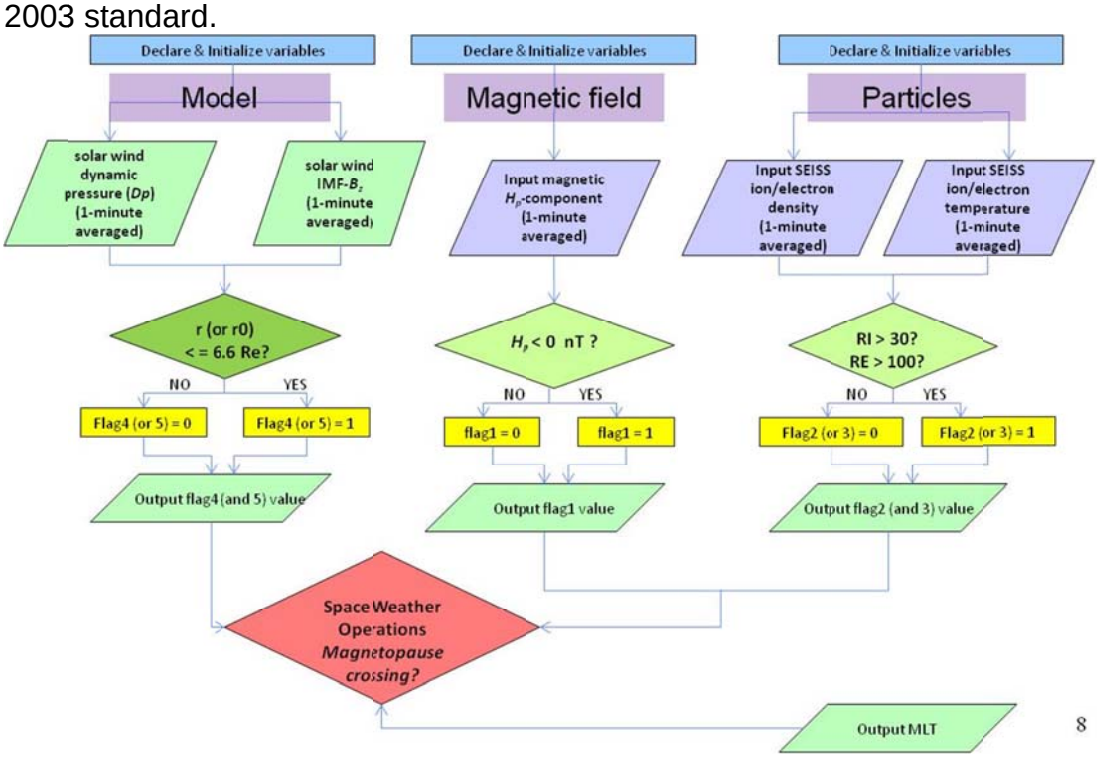

Figure 1 High-level flowchart of the GMC detection algorithm.

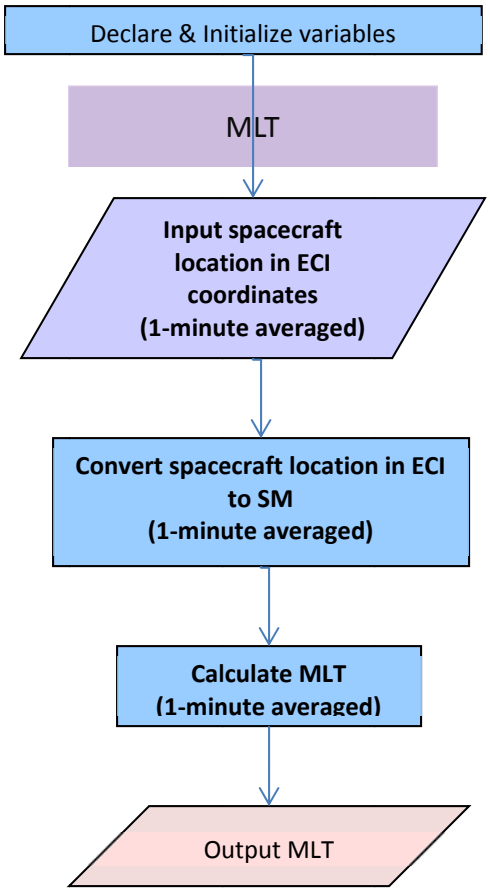

Figure 2 High-level flowchart of the magnetic local time (MLT) processing outline.

3.3 Algorithm Input

The algorithm requires GOES MAG and SEISS sensor data, solar wind data, spacecraft location and time tags. Input data requirements are summarized in tables 2 and 3.

3.3.1 Primary Sensor Data

Table 1 Sensor input data to the algorithm

Name	Description	Dimension
MAG	H_p-component sensor value in ENP coordinates	1-D (X)

SEISS	Ion temperature	keV
SEISS	Ion density	n/cm^3
SEISS	Electron temperature	keV
SEISS	Electron density	n/cm^3
Time	Data time tags	time series (hh,mm,ss.ss)
Date	Data date tags	time series (yy,mm,dd)
Spacecraft location	Spacecraft location in ECI coordinates (km)	3-D (X,Y,Z)

3.3.2 Ancillary Data

Table 2 Ancillary input data to the algorithm

Name	Description	Dimension
Solar wind pressure	Solar wind dynamic pressure	nPa
Solar wind IMF-B_z	Solar wind interplanetary magnetic field (IMF)-B_z component in GSM coordinates	nT
Solar wind speed	Solar wind speed	km/s

3.4 Theoretical Description

Very strong geomagnetic storms are often accompanied by compression of the magnetopause to altitudes below geosynchronous. Detection of geosynchronous magnetopause crossings indicate significant solar wind energy received at Earth and these strong storms can cause disruption to satellites, communications and

ground-based electrical systems. The physical and mathematical details of the algorithm are presented below.

3.4.1 Physics of the Problem

3.4.1.1 Magnetic signatures of geosynchronous magnetopause crossings

When a GMC occurs detection of the event by in-situ magnetometers are often best observed in the north/south magnetic field component. This is because the north/south component often turns from positive to negative during GMCs and there a very few other physical phenomena in the magnetosphere that would make the component turn negative. Storms that are signficiant enough to cause the magnetopause location to move to geosynchronous altitudes require a southward interplanetary magnetic field north-south component (IMF-Bz) to maximize magnetic reconnection of the IMF to the magnetopheric magnetic field on the dayside. An example of the in-situ GMC magnetic signature is shown in Figure 3 where the magnetic H_p –component (north-south) turns strongly negative due to the magnetopause moving to below the altitude of both GOES 6 & 7.

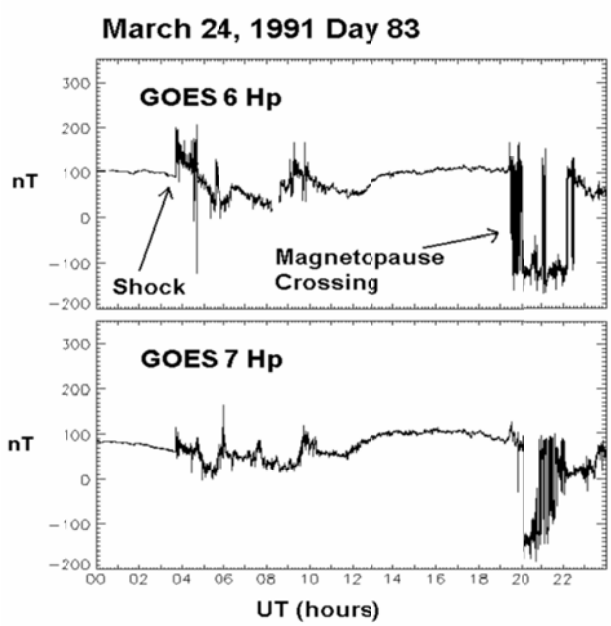

Figure 3 Shown is an example GMC detected by the GOES 6 & 7 magnetometers.

In this algorithm it is assumed that for the magnetic field component of the algorithm IMF-Bz is negative during GMCs and therefore that *Hp* is also negative during GMCs.

3.4.1.2 Particle signatures of geosynchronous magnetopause crossings

Particle signatures of GMCs are most often recognized by an increase in the mid-energy ion (or electron) density and a decrease in the same article temperatures. An example of this change in density and temperature is shown in Figure 4 below from the ISEE spacecraft. For this algorithm the ratio of density to temperature is used to define a GMC and the limit for this ratio is based on the work of Suvorova et al. (2005).

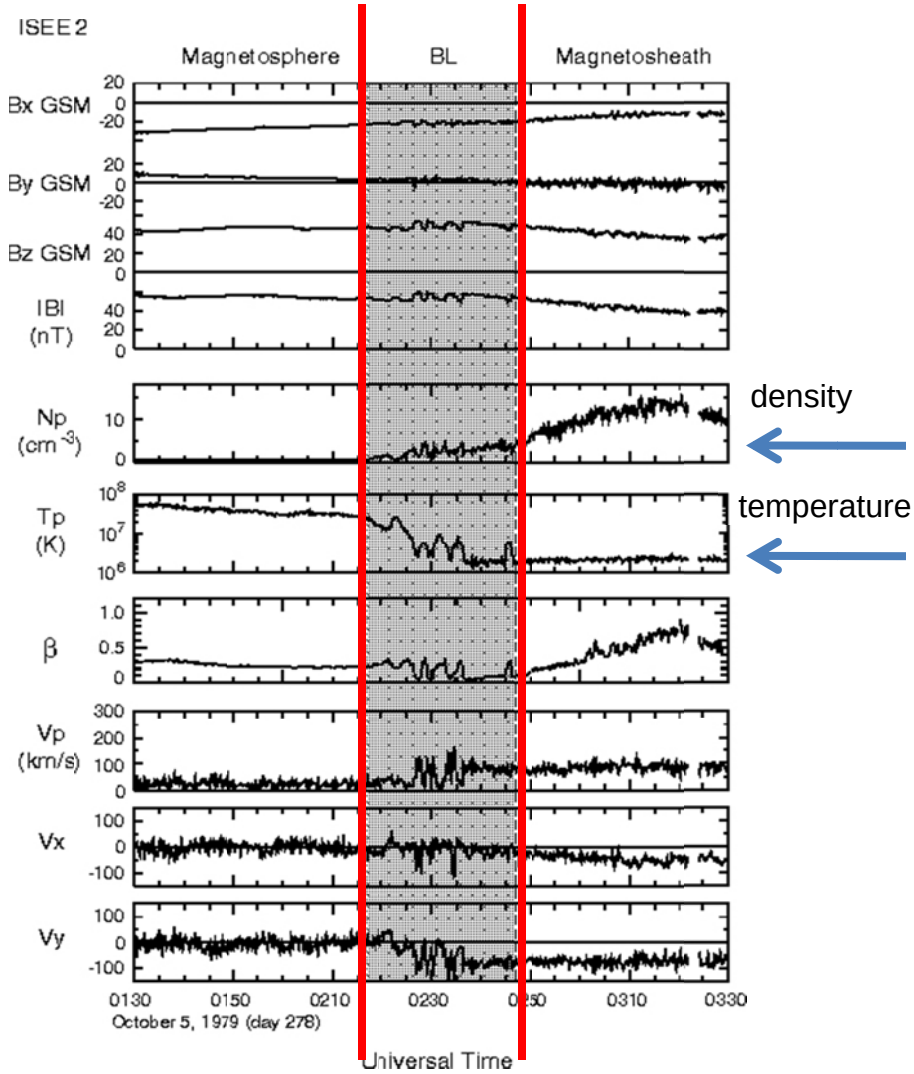

Figure 4 Shows the change is different parameters as the ISEE spacecraft moves from the magnetosphere to the magnetospheath (outside the magnetosphere). The density and temperature after the second vertical red line is significantly different to the values before the first red vertical line.

3.4.1.3 Magnetopause model

Three magnetopause models were tested to determine which was most suitable for inclusion in the algorithm. These were the Shue et al. (1998), Chao et al. (2001) and Petrinec and Russell (1996) models. All these models use solar wind IMF-Bz and solar wind dynamic pressure (Pdyn) and input. The models were developed using least squared fits of the solar wind parameters to

magnetopause location observed by multiple spacecraft. Some of the model development separated individual events by a minimum time interval, and restricted local time ranges while individually defining events. Here, we only restrict local time ranges and the model must run on 1-minute cadence data.

Using historical events observed by GOES and the corresponding solar wind data, results uing the different models are shown in Table 4. When using solar wind parameters within the valid ranges of the models, the Shue et al. (1998) model predicted ~57% of the events while Chao et al. (2001) and Petrinec and Russell (1996) models both predicted 0%. Hence, we use the Shue et al. (1998) model, which requires solar wind dynamic pressure and IMF-Bz as inputs.

Table 3 test results of comparisons between the three different magnetopause models.

Study	Points (minutes)	Year	No. SM Predicted	No. CM Predicted	No. PRM Predicted
Predictions for magnetopause location as defined by the vector from Earth through					
This study (SM)	1999	99-06	1130	-	-
This study (CM)	70	99-06	-	0	-
This study (PRM)	22	99-06	-	-	0
Yang et al. (2002)	1220	99-00	898	1027	1145
This study	563	99-00	321	322	396
This study	3856	99-06	1992	2463	2991
Predictions for magnetopause subsolar standoff distance r_0					
This study (SM)	1455	99-06	985	-	-
This study (CM)	49	99-06	-	0	-
This study(PRM)	21	99-06	-	-	0
This study	2451	99-06	1795	1865	2146

– within valid ranges for each model, between 08-16 MLT
– same time range as Yang et al., includes points outside each model's valid
– includes points outside each model's valid range, 06-18 ML

PRM – Petrinec and Russell (1996) Model
SM – Shue et al. (1998) Model
CM – Chao et al. (2001) Model
PoD – Probability of Detection (percent)

- Event defined by GOES H_p
- Calculated Probability of D
  2002)
  PoD = HT/(HT + MT), wher
  (occurrence) and MT is M

3.4.2 Mathematical Description

The algorithm consists of 3 components, the magnetic field, particle and model components. They are mathetically described below.

3.4.2.1 Magnetic field Component

The mathematical description is very simple with the condition

$H_p < H_{p_limit}$ (1),

defining a GMC. The value of H_{p_limit} is based on the correlation between H_p and IMF-B_z during GMCs. We assume GMCs occur only when IMF-B_z is negative, hence, H_{p_limit} = 0 nT.

3.4.2.2 Particle Component

We use the ratios limits defined by Suvorova et al. (2005)

D/T > 30 for the ion ratio (RI) and
D/T > 100 for the electron ratio (RE) (2)

3.4.2.3 Magnetopause model

The Shue et al. (1998) magnetopause model equations are

$$r = r_0 \left(\frac{2}{1+\cos\theta}\right)^{\alpha}$$

$$r_0 = \{10.22 + 1.29\tanh[0.184(B_z + 8.14)]\}(D_p)^{\frac{-1}{6.6}}$$

$$\alpha = (0.58 - 0.007B_z)\left[1 + 0.024\ln(D_p)\right] \quad (3)$$

where

- r is the magnetopause location along the Earth-satellite vector.
- r_0 is the magnetopause subsolar standoff distance along the Earth-sun line.
- θ the angle between Sun-Earth line and r.
- B_z is the IMF-Bz value in nT units.
- D_p is the solar wind dynamic pressure in nano-Pascal units.

The r-vector direction can be found by defining the GOES-R position unit vector $\mathbf{r_u(i,j,k)}$ as $\mathbf{r_u}=\mathbf{r_g}/r_g$, and assuming $\mathbf{k}$=0, $q=\cos^{-1}(\mathbf{i}/\mathbf{r_u})$, where r_g is the vector from center of Earth to GOES.

3.4.2.4 Coordinate Transformation

The input coordinate system for the Shue et al (1998) magnetopause model is aberrated GSM coordinates. The aberrated coordinates take into account Earth's orbital rotation around the Sun of ~30 km/s in the GSE coordinate system [e.g., Shue et al., 1998; Dmitriev et al., 2003]. the solar wind speed. Starting with the GSE coordinates [see, *magnetometer convert data to alternative geophysical coordinate systems, ATBD Version 1.0, 2008]* we convert to aGSE using

$$\theta_a = \tan^{-1}(30/Vsw)$$
$$G_{xagse} = G_{xgse}\cos\theta_a - G_{ygse}\sin\theta_a$$
$$G_{yagse} = G_{xgse}\sin\theta_a + G_{ygse}\cos\theta_a$$
$$G_{zagse} = G_{zgse}$$

where,

$$G_{iagse} \equiv \text{GOES - R location vector in aGSE coordinates (km), i = (x, y or z)}$$
$$Vsw \equiv \text{solar wind speed (km/s)}$$
$$G_{igse} \equiv \text{GOES - R location vector in GSE coordinates (km), i = (x, y or z)}$$

The aGSE to aGSM transformation is the same as GSE to GSM transformation [See, *magnetometer convert data to alternative geophysical coordinate systems, ATBD Version 1.0, 2008*]. As an example of this transformation, slower solar wind speed results in more aberration, for example, 400 km/s solar wind means about 4.3^o aberration.

3.4.2.5 Magnetic Local Time

The reliability of the algorithm will be dependent on the location of GOES-R during GMCs. We take this into account by outputting the magnetic local time (mlt) of GOES-R. The algorithm for mlt requires input of GOES-R location (x,y-components only) in SM coordinates and kilometer units. The Solar Magnetic (SM) Coordinate System is described in the Covert to Alternative Coordinate Transformation ATBD. The algorithm for seudo-code is

```
if x EQ 0 then
        if y LT 0 then
          theta=-90
if x EQ 0 then
  if y GT 0 then
    theta=90
      if x NE 0 then
  theta=tan-1(y/x)/p*180.0
      if x LT 0 and y GT 0 then
  theta=180+theta
        if x LT 0 and y LT 0 then
  theta=theta-180

     mlt=12/180*theta+12

if x LT 0 then
   if y EQ 0 then
     begin
       mlt=0
       theta=-180.0
     end
```

3.4.3 Algorithm Output

Table 4 Algorithm output

Name	Description	Dimension
Flag1	Set to 1 when magnetic field H_p-component is negative, else 0.	**integer**
Flag2	Set to 1 when ion density to temperature ratio is greater than 30, else 0.	**integer**
Flag3	Set to 1 when electron density to temperature ratio is greater than 100, else 0.	**integer**
Flag4	Set to 1 when magnetopause stand off distance *r* <= 6.6 *Re* from the	**integer**

	magnetopause model, else 0.	
Flag5	Set to 1 when magnetopause distance r_0 <= 6.6 *Re* from the magnetopause model.	**integer**
Magnetic local time	GOES-R magnetic local time (MLT)	**time series (hh.mmm)**

4.0 TEST DATA SETS AND OUTPUTS

4.1 Simulated/Proxy Input Data Sets

The proxy data for the magnetic field component of the algorithm uses previous GOES magnetic field data. For the SEISS instrument we use LANL data as previous GOES particle instrument data does not cover the range of energies required for the algorithm. Proxy particle data from LANL were found to work best when the LANL and GOES satellites were separated by 30 degrees or less.

4.2 Output from Simulated/Proxy Inputs Data Sets

Output examples from the algorithm using proxy data are shown in the figure below.

4.2.1 Output from MAG and SEISS simulated inputs data sets

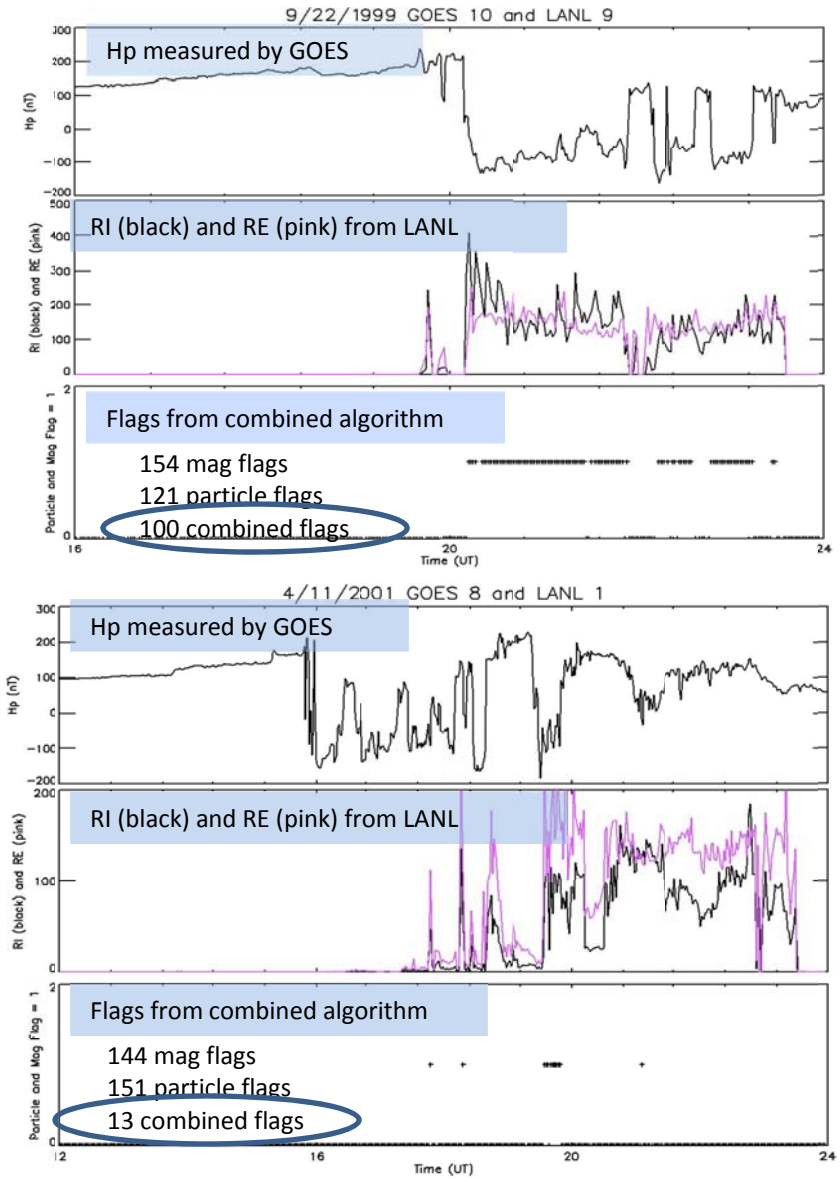

Figure 5 Output examples of two different GMC events when LANL and GOES were 30 degrees apart (top panels) and when LANL and GOES were 90 degrees apart. The number of particle flags that agree with magnetometer flags significantly decrease when the spacecraft are separated by 90 degrees.

- 09/22/1999
  - GOES 10 at approxi
    the start of the eve

- 04/11/2001
  - GOES 10 at approx
    the start of the ev

4.2.2 Output from magnetopause model tests

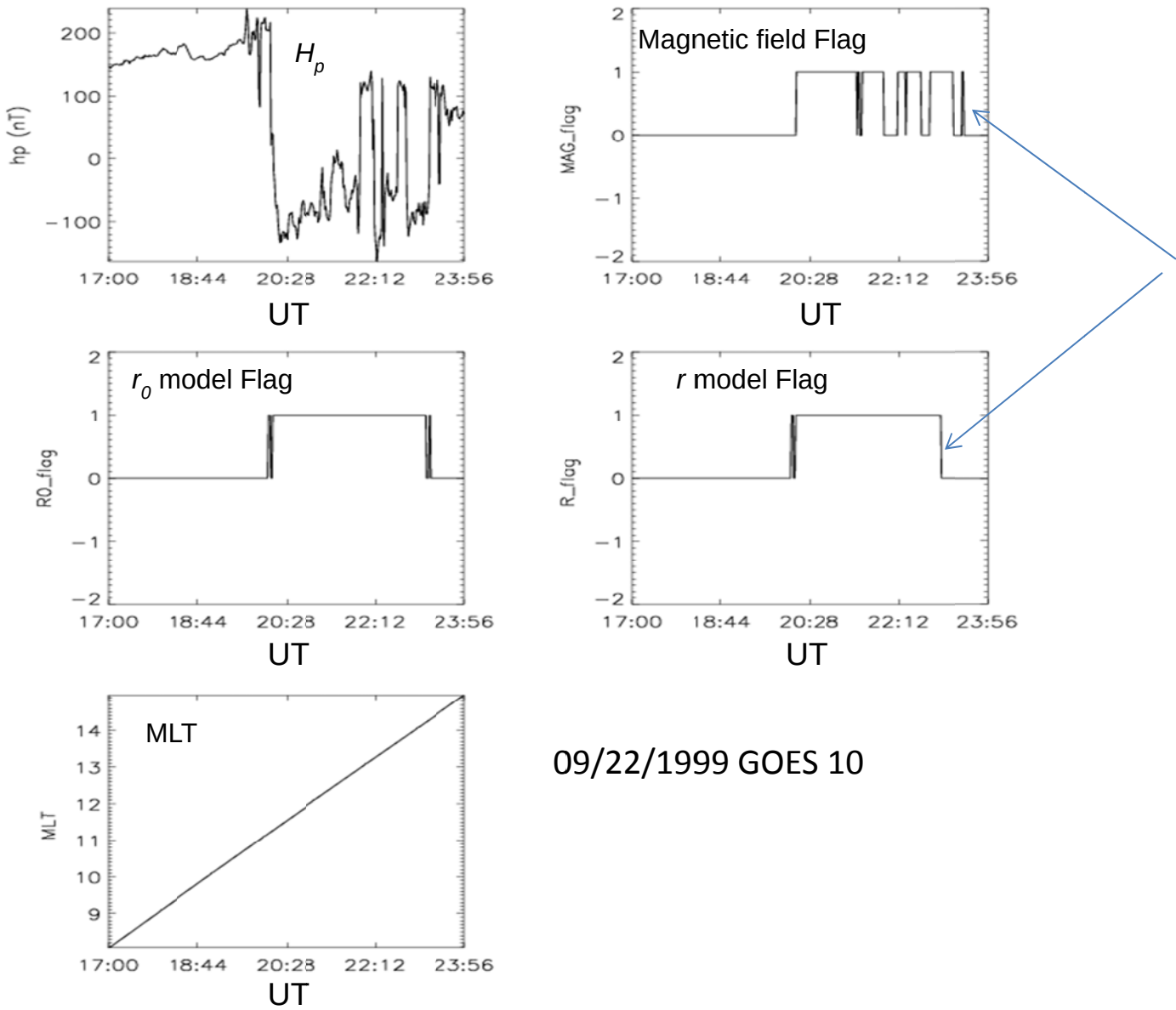

Figure 6 An output example from magnetopause model component of algorithm showing how the r-vector flags can disagree with magnetic field component of the algorithm.

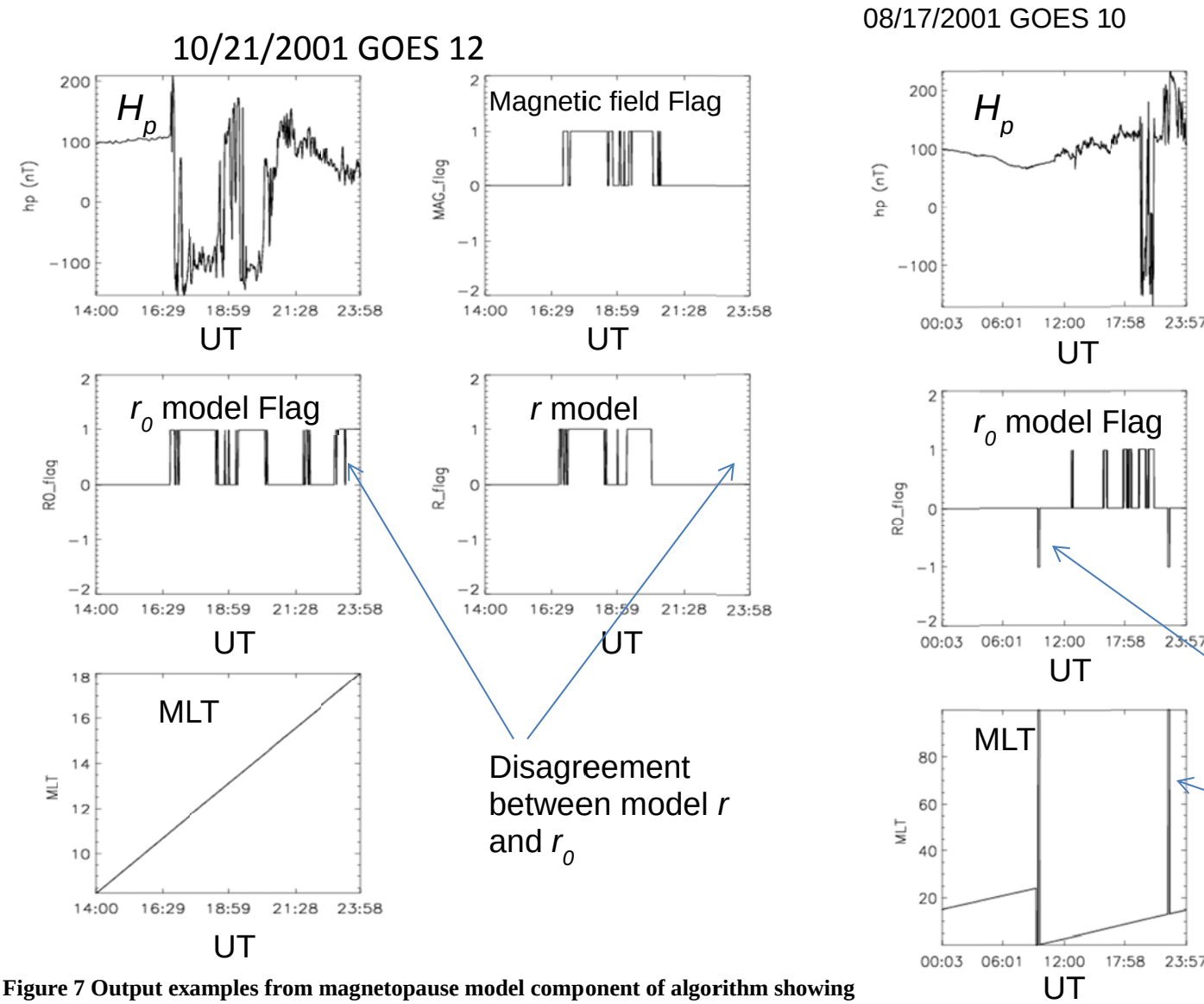

Figure 7 Output examples from magnetopause model component of algorithm showing in the r-vector flags (left panels) and errors in the flags.

4.2.3 Output example from full algorithm

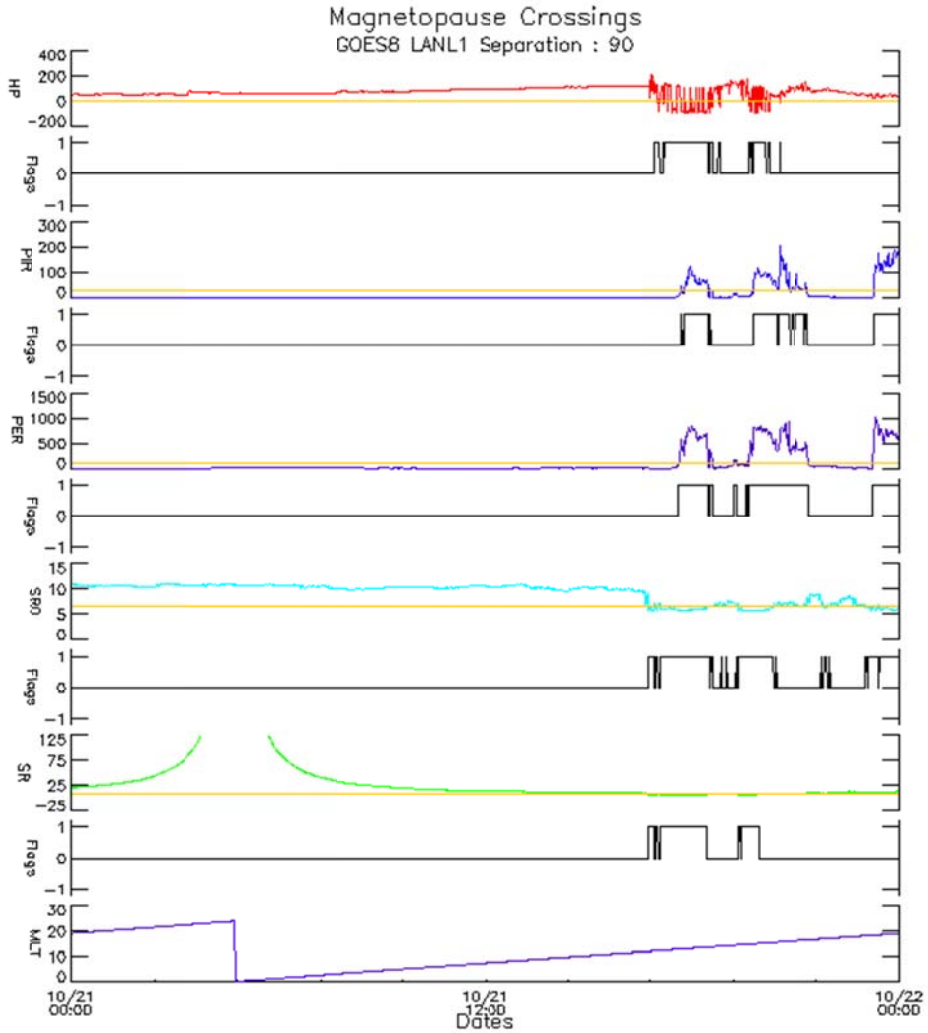

Figure 8 Example output with no errors. From top to bottom panels are HP the Hp-compnent of GOES magnetic field observations, magnetic field Flag, PIR is the ion density to temperature, ion ration event flag, PER is the electron density to temperature ratio, electron event flag, magnetopause model r_0-vector, r_0-vector event flag, magnetopause model r-vector, r-vector event flag and MLT.

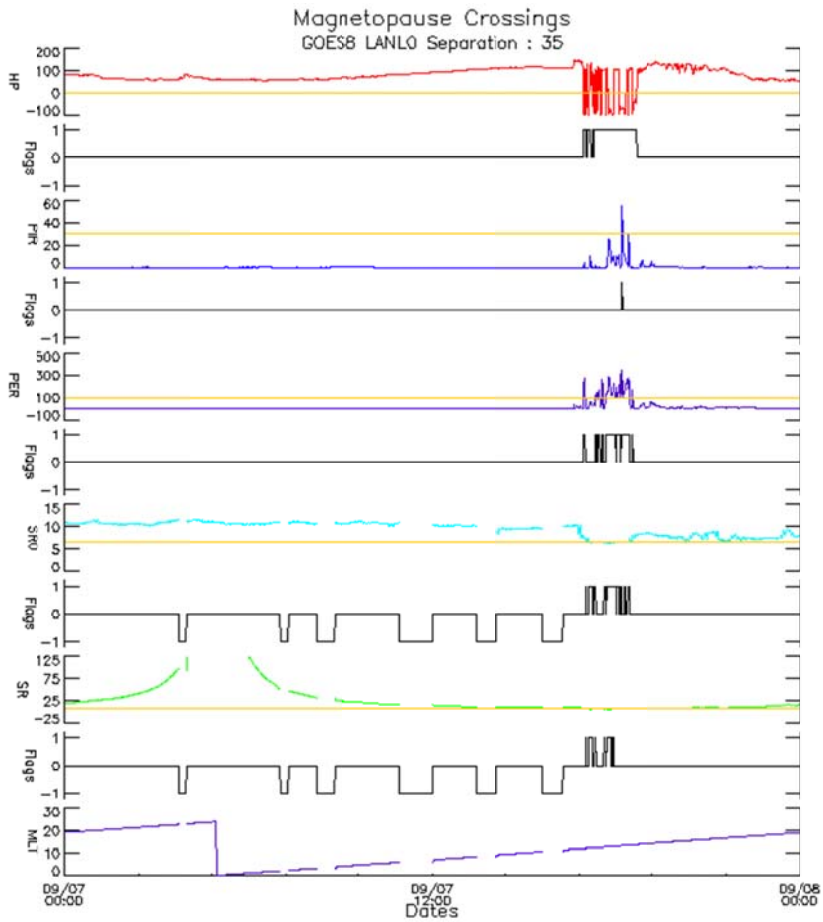

Figure 9 Example output with errors. From top to bottom panels are HP the Hp-compnent of GOES magnetic field observations, magnetic field Flag, PIR is the ion density to temperature, ion ration event flag, PER is the electron density to temperature ratio, electron event flag, magnetopause model r_0-vector, r_0-vector event flag, magnetopause model r-vector, r-vector event flag and MLT.

4.2.4 Precisions and Accuracy Estimates

The accuracy of the LANL data as proxy significantly decreases when LANL and GOES are separated by more than 35° longitude. The particle ratios appear to provide a good indicator of magnetopause crossings due to the strong correlation with magnetometer H_p-component. However, there are times when GMCs are observed outside the event criteria limits. The Shue et al. (1998) model was implemented correctly. When comparing to the magnetic field component of the algorithm the results seem consistent with expected results.

4.2.2 Error Budget

N/A

5.0 PRACTICAL CONSIDERATIONS

There are many practical considerations in this algorithm with some not yet idenfified explicitly. For example, the spacecraft location is required to determine the magnetopause location along the Earth-satellite vector and to calculate magnetic local time. Also, the assumed magnetic field coordinate system is ENP, however, the ENP system is not currently well defined at Level 1B. Furthemroe, the GOES field in GSM coordinates is more optimal for correlation with IMF-B_z.

In addition, continuous 1-minute solar wind dynamic pressure and IMF-B_z data are required for model, as well as continuous 1-minute electron and ion moments data. We assume that the magnetic field H_p-component value represents GMC truth, but this is very difficult to verify for 100% of the events. There has also been no consideration given to how the output should be displayed.

The algorithm also assumes the solar wind data are accurate to within the 1-minute resolution of the output. This includes assuming that the propagation of the solar wind data from L1 to Earth is accurate within the 1-minute resolution of the data. It has also not been determined how the solar wind will be made available as a realtime stream to the algorithm.

Finally, we have not fully tested the algorithm under different scenarios to understand other possible practical considerations. The algorithm should probably run on a proving ground type environment before going fully operational.

5.1 Numerical Computation Considerations

There are no foreseeable computational issues.

5.2 Programming and Procedural Considerations

The algorithm essentially runs as a state machine. When a GMC is detected the state switches to on (or 1), otherwise the state is zero (or off). As previously mentioned, there has been no consideration given to the how to display the states of the algorithm for forecasters.

5.3 Quality Assessment and Diagnostics

The following procedures are recommended for diagnosing the performance of the algorithm.

- Compare results to research community publications.
- Compare results to near by spacecraft.

5.4 Exception Handling

Member functions will return 0 or 1 with 0 meaning no error and 1 meaning an error occurred. However, in most functions no action is taken as a result of an error return. The input data are assumed to have error flags represented by fill in values. If the input value to the algorithm, that is nedded to calculate a flag, is a fill in value, then that corresponding output event flag is set to -1. However, no other exception action is taken given an error.

5.5 Algorithm Validation

Pre-Launch Validation:

The algorithm will be/has been validated as described in section 4 by comparisons to research community results and nearby spacecraft.

Post-Launch Validation:

The algorithm will be validated by comparing output to research community results and near-by spacecraft.

6.0 ASSUMPTIONS AND LIMITATIONS

6.1 Performance

The algorithm assumes that solar wind data are always available in real-time (within 1-minute). The requirement of 90% events detected with false detection 10% of the time has not been validated. The algorithm assumes GMCs occur only when Hp is < 0 nT and positive Hp events have not been studied. The ion and electron ratio Probability of Detection has not been esitmated.

However, it should be noted that the algorithm is significantly better than any previously implemented magnetopause crossing detection algorithm.

6.2 Assumed Sensor Performance

The algorithm assumes the GOES-R magnetometer and SEISS sensors will meet specification and performance requirements within normal operational parameters. The algorithm assumes that time tags are accurate and that GOES-R spacecraft location data will be available in real time. The algorithm also assumes the solar wind data are accurate to within the 1-minute resolution of the output. This includes assuming that the propagation of the solar wind data from L1 to Earth is accurate within the 1-minute resolution of the data.

6.3 Pre-Planned Product Improvements

6.3.1 Improvement 1

The algorithm requires verification and validation under simulated or real operational conditions. For example, testing in an environment such as the proving ground would be very valuable. In particular it would allow us to determine if model limits should be widened to include events outside valid ranges and $H_p > 0$ nT events.

6.3.2 Improvement 2

A study of the possibility of using the GOES magnetic field Bz-GSM component instead of ENP H_p-component would be highly valuable.

6.3.3 Improvement 3

A study should be undertaken to determe the Probability of Detection for ion and electron moment ratios as well as determining if the particle event criteria need modification.

6.3.4 Improvement 4

Further testing is required of the model output and applicability, for example, determing the accuracy of the r_0-vector when GOES-R is in the nightside.

6.3.5 Improvement 5

A study that looks at combining event flags to create different confidence levels for the forecaster would be useful, in addition to a study of the visualization of the output from the algorithm.

6.3.6 Improvement 6

More extensive exception handling is required.

7.0 REFERENCES

(1) Suvorova A., A. Dmitriev, J.-K. Chao, M. Thomsen, Y.-H. Yang (2005), Necessary conditions for geosynchronous magnetopause crossings, J. Geophys. Res., 110, A01206, doi:10.1029/2003JA010079.

(2) Dmitriev A., J.-K. Chao, M. Thomsen, A. Suvorova (2005), Geosynchronous magnetopause crossings on 29–31 October 2003, J. Geophys. Res., 110, A08209, doi:10.1029/2004JA010582.

(3) Lopez R. E., S. Hernandez, M. Wiltberger, C.-L. Huang, E. L. Kepko, H. Spence, C. C. Goodrich, J. G. Lyon (2007), Predicting magnetopause crossings at geosynchronous orbit during the Halloween storms, Space Weather, 5, S01005, doi:10.1029/2006SW000222.

(4) Dmitriev A. V., A. V. Suvorova, J. K. Chao, Y.-H. Yang (2004), Dawn-dusk asymmetry of geosynchronous magnetopause crossings, J. Geophys. Res., 109, A05203, doi:10.1029/2003JA010171.

(5) Chao, et al., Cospar Colloquia Ser., vol. 12, pp. 127– 134, 2002.

(6) Dmitriev et al., JGR, A05203, doi:10.1029/2003JA010171, 2004.

(7) Dmitriev, et al., JGR, 108(A12), 1464, doi:10.1029/2003JA010027, 2003.

(8) Farris and Russell, JGR, p.17681, 1994.

(9) McComas et al, JGR, p. 21249, 1994.

(10) Petrinec and Russell, JGR, p. 137, 1996.

(11) Shue et al., JGR, p.17691, 1998.

(12) Le et al., JGR, 99, 23,723-23,734, 1994

(13) Loto'aniu, et al., The GOES-R magnetometer coordinate transformation theoretical basis document, NOAA-NESDIS publication, 2008.

(14) Rodriguez et al., SEISS Moments CDR, 2010.

(15) Yang et al., JGR, 108, , 1104, doi:10.1029/2002JA009621, 2003.